Mathematical Biosciences and Engineering

MBE, 20(2): 2482–2500.
DOI: 10.3934/mbe.2023116
Received: 28 September 2022
Revised: 05 November 2022
Accepted: 11 November 2022
Published: 22 November 2022

http://www.aimspress.com/journal/MBE

Research article

A multi-feature fusion decoding study for unilateral upper-limb fine motor imagery

Liangyu Yang[1], Tianyu Shi[1], Jidong Lv[1], Yan Liu[2, 3], Yakang Dai[2, 3,*] and Ling Zou[1, 4,*]

[1] The School of Microelectronics and Control Engineering, Changzhou University, Changzhou, Jiangsu 213164, China
[2] Suzhou Institute of Biomedical Engineering and Technology, Chinese Academy of Science, Department of Medical Image, Suzhou 215163, China
[3] Suzhou Guokekangcheng Medical Technique Co., Ltd., Suzhou 215163, China
[4] Key Laboratory of Brain Machine Collaborative Intelligence Foundation of Zhejiang Province, Hangzhou, Zhejiang 310018, China

* **Correspondence:** Email: zouling@cczu.edu.cn, daiyk@sibet.ac.cn.

Abstract: To address the fact that the classical motor imagination paradigm has no noticeable effect on the rehabilitation training of upper limbs in patients after stroke and the corresponding feature extraction algorithm is limited to a single domain, this paper describes the design of a unilateral upper-limb fine motor imagination paradigm and the collection of data from 20 healthy people. It presents a feature extraction algorithm for multi-domain fusion and compares the common spatial pattern (CSP), improved multiscale permutation entropy (IMPE) and multi-domain fusion features of all participants through the use of decision tree, linear discriminant analysis, naive Bayes, a support vector machine, k-nearest neighbor and ensemble classification precision algorithms in the ensemble classifier. For the same subject, the average classification accuracy improvement of the same classifier for multi-domain feature extraction relative to CSP feature results went up by 1.52%. The average classification accuracy improvement of the same classifier went up by 32.87% relative to the IMPE feature classification results. This study's unilateral fine motor imagery paradigm and multi-domain feature fusion algorithm provide new ideas for upper limb rehabilitation after stroke.

Keywords: brain-computer interface; upper limb rehabilitation; unilateral fine motor imagery; multi-domain fusion

1. Introduction

Stroke is a brain deficit-causing condition caused by ischemic or hemorrhagic injury to the brain. According to the World Health Organization, stroke is the second leading cause of death worldwide [1]. Approximately one-third of patients have upper limb motor deficits after treatment [2]. Rehabilitation training for stroke patients includes forced exercise, transcranial direct current stimulation, robotic therapy, mirror therapy [3], stem cell therapy and drug therapy [4]. However, passive training and treatment cannot reshape the patient's brain nerves [5], and the emergence of motor imagery brain-computer interfaces (MI-BCIs) has dramatically improved current methods of upper limb rehabilitation training for post-stroke patients [6]. At present, most motor imagery-based brain-computer interfaces (BCIs) are in the laboratory research stage, and the participants are primarily healthy individuals [7].

The traditional stroke rehabilitation training paradigm design is minimal and was developed from left- and right-hand to limb rehabilitation training, but these rehabilitation training paradigms are ineffective. Khalaf et al. [8] designed a left- and right-hand rehabilitation training paradigm with left and right direction arrows appearing randomly on the screen for 10 s each time for 150 training sessions. Gaur et al. [9] designed a four-category motor imagery rehabilitation paradigm that included the left and right hands, lower limb and tongue. Each subject had two phases, training and testing at different times, and each training session included four sessions with 72 trials each. By training different joints of a single limb, more brain areas can be activated to work and improve the effectiveness of rehabilitation training.

Brain activation of subjects during motor imagery training can be found by obtaining electroencephalography (EEG) signal features of the corresponding paradigm. In the past decades, feature extraction algorithms for motor imagery have made huge progress [10], and common spatial pattern (CSP) [11], filter bank CSP [12] and short-time Fourier transform [13] are widely used in the decoding research of motor imagery. The use of a wavelet transform and fast Fourier transform [14] constitute early methods used for motor imagery EEG (MI-EEG) time domain analysis to directly extract features such as average and peak values of EEG signals [7]. Methods such as mean frequency [15] and median frequency [16] were used to analyze the EEG rhythm of MI-EEG from the perspective of the frequency domain. Because of the nonlinear characteristics of EEG [17], entropy domain algorithms such as Shannon entropy [18] and sample entropy [19] have also been used to extract MI-EEG features. When subjects imagine the movement of different limbs and joints, the rhythm of the sensorimotor area of the brain changes significantly so that the CSP algorithm can analyze the MI-EEG features from the perspective of the spatial domain [20, 21].

Feature extraction methods from different perspectives have their individual advantages and, at the same time, their own limitations. Time and frequency domain methods are simple and effective, but they become less and less valuable when the complexity of the data increases [22]. Entropy-domain features can analyze EEG from a nonlinear perspective, but the processing time is too long. The spatial domain algorithm is sensitive to MI-EEG, but it does not work well when the number of channels is too small. For the collected ipsilateral limb motor imagery-paradigm EEG data, the classification accuracy of the above methods needs to be improved.

Yu et al. [23] proposed an improved lightweight feature fusion network to achieve a classification effect with an average Kappa value of 0.881 for the dataset of the BCI competition IV 2a. Wang et al. [24] proposed a novel MI-EEG classification method by combining Shannon complex wavelet and

convolutional neural networks. The Kappa value of this method for the BCI competition IV 2a dataset was 0.704.

Most post-stroke patients with hemiplegia have dysfunction in only one limb, while most of the classical motor imagery paradigms used in MI-BCI rehabilitation involves bilateral motor training of the right and left hands [25], and limb training on the healthy side does not work for the rehabilitation of the affected limb.

In order to meet the specific needs of post-stroke hemiplegic patients, we designed a fine motor imagery paradigm with unilateral focus on elbow and shoulder joints. The unilateral training of specific joints is more complex than bilateral limb training, as it can activate more brain areas and better meet the rehabilitation needs of hemiplegic patients. Then, based on the advantages of different extraction methods and the characteristics of fine motor imagination, a multi-feature fusion method combining the spatial domain CSP algorithm with the improved multiscale permutation entropy (IMPE) algorithm in the entropy domain is proposed.

2. Materials

2.1. Subjects

Here, the study of single-limb fine motor imagery and its feature extraction was in the laboratory stage. Twenty healthy right-handed subjects (18 males and 2 females, aged 20–26 years) with normal or corrected normal vision and no previous history of stroke or genetic history were selected for the experiment. Before the experiment, the paradigm process was explained to all subjects in detail. At the end of the experiment, the subjects were asked about their feelings about the experiment to ensure that the motor imagery training was adequately performed. All experiments on human subjects were conducted in accordance with the Declaration of Helsinki, and all subjects were approved by the Ethics Committee of Changzhou University.

2.2. Experimental paradigm

The experimental paradigm was written in JavaScript. As shown in Figure 1, the subjects placed their hands naturally on their thighs, and their eyes were 1 m away from the screen. At the beginning of each training session (8 s), a white cross in the center of the display for 2 s cued the subject's attention to an upcoming target. The target cue ("shoulder" or "elbow") appeared on the screen for 4 s. During this process, the subject visualized the cued action (right shoulder abduction or 90° elbow flexion) in their mind. The experiment was divided into three sessions, with each subdivided into 40 training trials (320 s), and two motor imagery tasks were performed in each experimental phase (the different movements were required to appear 20 times).

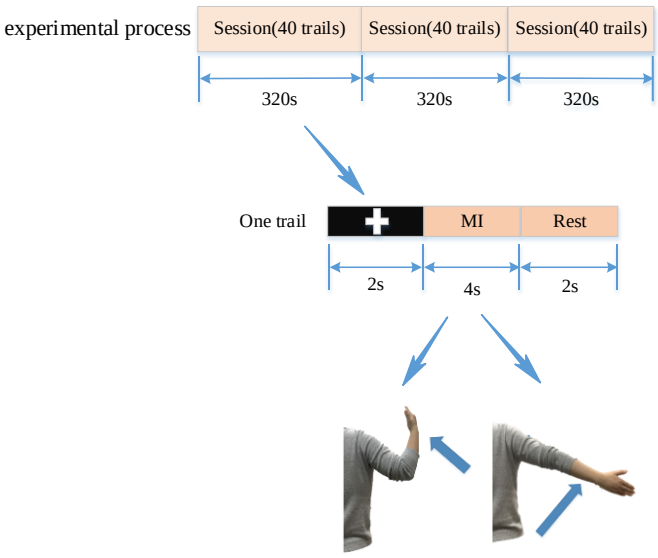

Figure 1. Unilateral fine motor imagery paradigm flow.

2.3. Data acquisition

The data acquisition device was a Neuracle NeuSen W series wireless EEG acquisition system (64 channels), which has the advantages of high portability, a stable signal and good shielding. The electrode positions of NeuSen W series were arranged according to the International 10–20 system, and the sampling rate of the device was 1000 Hz. Among them, the 59–64 leads were ECG, HEOR, HEOL, VEOU and VEOL. In subsequent data processing, the data of these five leads needed to be deleted, so the actual EEG data comprised 59 leads.

3. Methods

The process used in this study is shown in Figure 2, where the raw EEG of the unilateral fine-motor imagery paradigm was first acquired with a Neuracle 64-channel EEG cap. The raw EEG data were then denoised with a band-pass filter (8–30 Hz), re-referenced, analyzed via independent components analysis (ICA) and segmented. Then, the CSP and IMPE features were extracted from the pre-processed EEG data. Second, the CSP feature matrix and IMPE feature matrix were fused with features and the fused matrix was filtered with features. Finally, the filtered features were put into the classical classifier for classification to obtain the optimal classification accuracy for unilateral fine motion imagery. Figure 2 explains the specific process of the experiment in this study, highlighting the fusion of two features after the feature extraction of fine motor imagery EEG so as to achieve better classification accuracy.

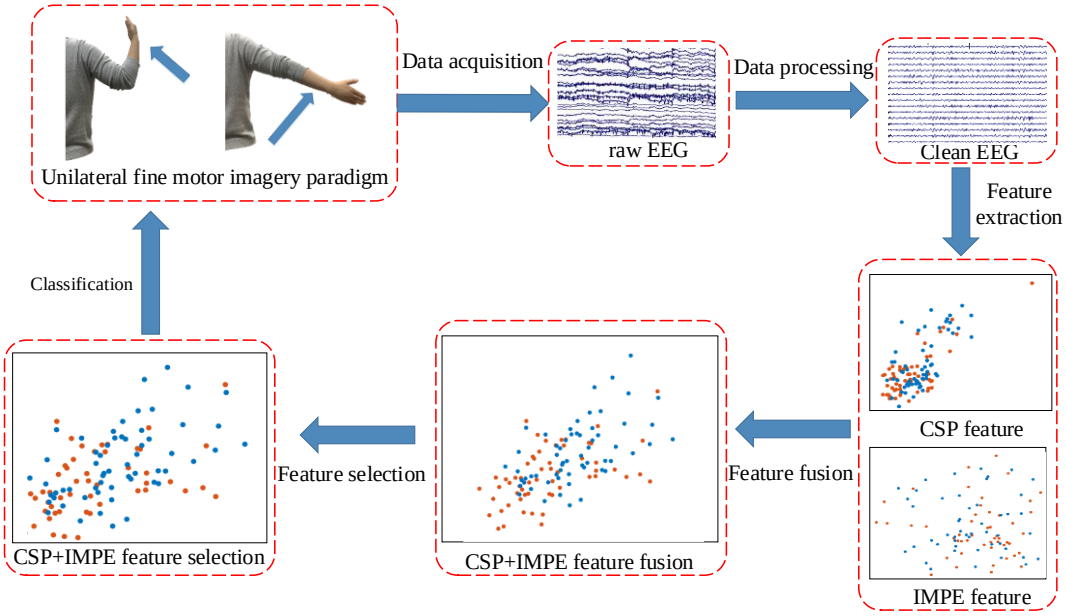

Figure 2. Unilateral fine motor imagery data preprocessing and feature extraction.

3.1. Data preprocessing

EEG data have noise interference such as electrooculography (EOG), eye movement, head movement and electrocardiography (ECG) signals, which affect the reliability of the extracted motor imagery features. Therefore, EEG data need to be preprocessed before feature extraction. The preprocessing of EEG data in this study involved the use of eeglab v2021.1, but the EEG data collected by the Neuracle device was in the bdf format; and, the "From Neuracle EEG data files" plugin needed to be updated in eeglab. First, unwanted 59–64 channels were removed from the original EEG data. Second, the data were filtered at 8–30 Hz. Then, ICA analysis was performed to remove noise, such as EOG, eye movement, head movement and ECG signals, from the EEG data. Finally, the data treated with ICA was segmented with a range of 0–4 s.

3.2. Common spatial pattern feature extraction

CSP is a spatial filtering feature extraction algorithm for two classification tasks, extracting the spatial distribution components of each category from multi-channel EEG data [26]. The CSP algorithm aims to design a spatial filter to maximize the difference between the variance values of the two groups of EEG spatiotemporal signal matrices after filtering to obtain a feature vector with high discrimination. For the next step, the feature vectors are sent to the classifier for classification [27].

Given that two different fine motor imagery EEG data segments were set as X_1 and X_2, the normalized covariance matrix of X_1 and X_2 is

$$R_{1,i} = \frac{X_{1,i}X_{1,i}^T}{trace(X_{1,i}X_{1,i}^T)} \tag{3.1}$$

$$R_{2,i} = \frac{X_{2,i}X_{2,i}^T}{trace(X_{2,i}X_{2,i}^T)} \tag{3.2}$$

where $trace(\bullet)$ is the sum of elements on the diagonal of the matrix, i is the number of trails in the EEG data, the data dimension of X_1 and X_2 is $N \times S$, N is the number of EEG channels and S is the number of data points of each trial.

Perform w-space filtering on the input data $X_{N\times S}$:

$$Z_{2m\times s} = w_{2m\times s} X_{N\times S} \tag{3.3}$$

where $2m$ is the number of eigenvalues taken by the eigenmatrix.

The fine motor imagery features are calculated as shown in Eq (3.4):

$$f_p^i = log\left(\frac{var_p^i}{\sum_{p=1}^{2m} var_p^i}\right) \tag{3.4}$$

var_p^i is the variance of line p in $Z_{2m\times s}$, and integrating every f_p^i into f^i yields the motor imagery feature of each trial.

3.3. IMPE feature extraction

Multiscale permutation entropy (MPE) involves the addition of coarse-grained based on permutation entropy, and the entropy value can be obtained as a function of the time scale [28]; Azami et al. [29] introduced the IMPE to overcome the asymmetry of coarse-grained time series and the defects of the large time scale of MPE.

3.3.1. Permutation entropy

The collected unilateral fine motor imagery EEG data were divided into the time series $\{x_i\}_{i=1,\dots N}$, where N is the number of time points, and a vector containing d points was constructed, as shown in Eq (3.5):

$$x_t^{d,l} = \{x_t, x_{t+l}, \dots, x_{t+(d-2)l}, x_{t+(d-1)l}\} \tag{3.5}$$

where d is the embedding dimension and l is the time delay.

The permutation entropy is calculated as follows:

$$PE_x^{d,l} = -\sum_{i=1}^{d!} p(\pi_i) ln\big(p(\pi_i)\big) \tag{3.6}$$

where $p(\pi_t)$ is the relative frequency.

The d value is positively correlated with the sorted data, which increases the computation time while obtaining accurate results. Therefore, to compensate for the sorting amount and computation time, the value of d is usually set to 3, and the time delay l is usually set to 1 [30].

3.3.2. MPE

By introducing "coarse-grained" into the time series, the scaling factor can be obtained by averaging the time data points within a non-overlapping window with the length τ increasing.

Each element $j^{(\tau)}$ of the coarse-grained time series y is defined as [28]

$$y_j^{(\tau)} = \frac{1}{\tau}\sum_{i=(j-1)\tau+1}^{j\tau} x_i\,, 1 \le j \le \lfloor\frac{N}{\tau}\rfloor \tag{3.7}$$

Each coarse-grained time series has the length $\lfloor\frac{N}{\tau}\rfloor$. The second step is to compute the permutation entropy for each coarse-grained time series.

3.3.3. IMPE

MPE is asymmetric, and the results of MPE calculation have variability in long time scales, so the MPE needs to be improved. The IMPE is calculated as follows:

$z_i^{(\tau)} = \{{y_{i,1}}^{(\tau)}, {y_{i,2}}^{(\tau)}, \ldots, {y_{i,n}}^{(\tau)}\}$ generates the position ${y_{i,j}}^{(\tau)} = \frac{\sum_{f=0}^{\tau-1} x_{f+i+\tau(j-1)}}{\tau}$, and for each τ, we get τ different time series: $z_i^{(\tau)}|(i = 1, \ldots, \tau)$.

The permutation entropy is calculated separately for each $z_i^{(\tau)}|(i = 1, \ldots, \tau)$, and then the value of the IMPE is the average value of all permutation entropy (PE) values:

$$IMPE(x, \tau, d) = \frac{1}{\tau}\sum_{i=1}^{\tau} PE\left(z_i^{(\tau)}\right) \tag{3.8}$$

3.4. Multi-domain feature fusion algorithm

After pretreatment of the original EEG data, EEG features need to be extracted to explore the training effect of the unilateral fine motor imagery paradigm on the affected limb of patients after a stroke. Most current feature extraction algorithms are single-domain feature extraction algorithms, such as the time domain-, frequency domain-, space domain- and entropy domain-based algorithms. Although the time and frequency domains can significantly improve the speed of feature extraction, the complexity of EEG data induced by unilateral fine motor imagery is higher than that of classical left-handed motor imagery. Considering only the time and frequency domains, the extracted features' reliability is not high. CSP algorithms in the spatial domain are widely used in the field of motor imagery. CSPs can distinguish different movements by maximizing the variance of EEG signals under different labels. However, as the number of EEG channels decreases, the effect of CSP algorithms will drop. The entropy domain algorithm can find the subtle changes in EEG signals, and it has been widely used in EEG signal feature extraction. Among them, the IMPE algorithm improves the reliability of entropy. However, it takes too long for the entropy domain algorithm to operate, making the feature extraction time cost too high. Moreover, the classification accuracy is generally low when the entropy domain algorithm is used alone.

In this study, the features of unilateral fine motor imagery EEG data were extracted from the perspective of different domains, and the advantages of the algorithms in each domain were absorbed to make up for the defects of the algorithms in other domains. Because the EEG data used in this study consisted of 59 channels and each channel had 120 trails, the data complexity was very high, so the time domain and frequency domain algorithms cannot achieve a noticeable classification effect. This study involved combining the CSP algorithm in the spatial domain and the IMPE algorithm in the entropy domain. The high sensitivity of the CSP to motor imagery feature extraction made up for the low sensitivity and high time cost when IMPE was used alone, and the reliability of IMPE made up for the inadaptability of the CSP when the number of channels was negligible. The multi-domain

feature extraction algorithm proposed in this paper integrated the CSP and IMPE to complement their advantages. It has achieved good results on self-developed EEG signals of the unilateral fine motor imagery paradigm.

3.5. Feature outlier detection

After extracting the EEG features of unilateral fine motor imagery, the feature matrix has features with significant errors or redundancy, so it is necessary to detect the outliers in extracted features so as to remove those affecting the classification accuracy.

The k-nearest neighbor (KNN) algorithm prejudges unknown category samples by searching for the nearest k known category samples. The detection of outliers in KNN involves calculating the average distance between each sample point and its nearest k samples, and then comparing the calculated distance with the threshold. If it exceeds the threshold, it is considered as an outlier. The quantile calculation method was used to calculate the threshold value.

4. Results

4.1. CSP feature extraction and classification results

According to the CSP algorithm, the self-collected unilateral fine motor imagery EEG data used in this study had 59 channels and 120 trials, so m in the CSP algorithm was set to 11, that is, the first 11 lines and the last 11 lines of the spatial filter. Therefore, the dimensions of the CSP feature matrix were 120 × 22. In order to reduce the data dimension and improve the classification rate, it is necessary to delete some feature outliers; thus, the screened feature matrix was put into six classifiers for training and classification, namely, decision tree (Tree), linear discriminant analysis (LDA), naive Bayes, support vector machine (SVM), KNN and ensemble classifiers. Ten-fold cross-validation was used for classification. Table 1 shows the CSP feature classification results for the unilateral fine motor imagery EEG data of 20 healthy subjects. The bold part of the table shows the highest classification accuracy of different participants for different classifiers.

Table 1. Classification accuracy of CSP features for various classifiers (unit: %).

Participants	Tree	LDA	Naive Bayes	SVM	KNN	Ensemble
Sub01	69.2	91.7	82.5	**94.2**	89.2	**94.2**
Sub02	70	77.5	69.2	**88.3**	80	80.8
Sub03	67.5	74.2	65.8	**80.8**	69.2	69.2
Sub04	80	94.2	89.2	95.8	94.2	**96.7**
Sub05	69.2	79.2	69.2	**90**	77.5	**90**
Sub06	67.5	76.7	74.2	**80.8**	79.2	80
Sub07	66.7	80	68.3	80	74.2	**81.7**
Sub08	73.3	**98.3**	96.7	**98.3**	**98.3**	**98.3**
Sub09	78.3	85.8	79.2	**86.7**	**86.7**	**86.7**
Sub10	77.5	**84.2**	71.7	82.5	75.8	80.8
Sub11	70	**92.5**	80	90.8	85.8	88.3

Continued on next page

Sub12	71.7	86.7	81.7	**89.2**	83.3	87.5
Sub13	70.8	**95**	75	**95**	89.2	93.3
Sub14	75.8	89.2	85	**91.7**	85	90
Sub15	74.2	94.2	90	**95.8**	92.5	94.2
Sub16	83.3	90	85	**93.3**	84.2	92.5
Sub17	74.2	97.5	90	**98.3**	94.2	**98.3**
Sub18	67.5	89.2	78.3	**92.5**	87.50	**92.5**
Sub19	65	82.5	62.5	80.8	76.7	**83.3**
Sub20	73.3	79.2	75	**87.5**	80	83.3
Mean	**72.25**	**86.89**	**78.43**	**89.62**	**84.14**	**88.08**

Figure 3 shows the average classification accuracy of the CSP features of all subjects for the six classifiers.

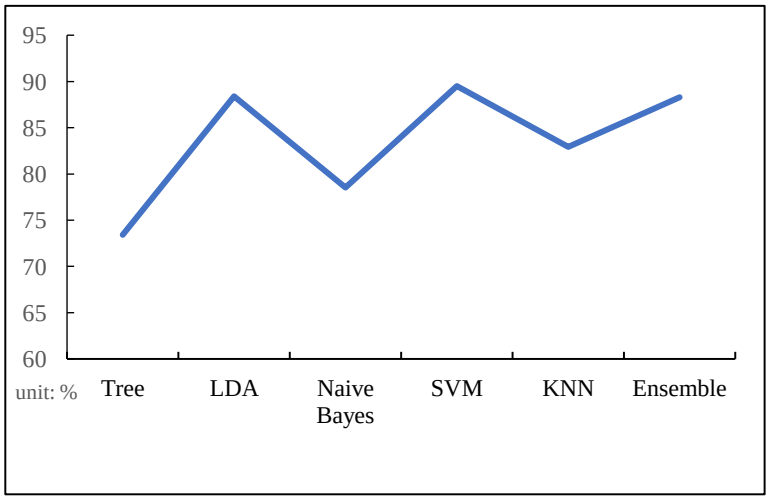

Figure 3. Average classification accuracy of CSP features for all subjects.

According to the classification results, Subject 8 achieved the highest classification accuracy of 98.3%, while Subject 6 achieved only 80.8%. The highest classification accuracy of a single subject was mainly focused on the SVM classifier. Meanwhile, the average classification accuracy of the SVM classifier was also the highest, reaching 89.62%. Therefore, the CSP algorithm and SVM classifier can achieve good classification accuracy on the unilateral fine motor imagery of two actions, but there is still much room for improvement.

4.2. IMPE feature extraction and classification results

The embedding dimension d affects the IMPE feature extraction when calculating the permutation entropy value, so either $d! \leq N$ or $(d+1)! \leq N$ should be used [26]. The value of d will affect the result of feature extraction. When d is too large, the calculation time will be very long. When the IMPE algorithm was used in this study, the order of permutation entropy was set to 3, the scale factor was set to 3 and the time delay was set to 1. The feature matrix after screening outliers was put into six classifiers for training and classification, namely, Tree, LDA, Naive Bayes, SVM, KNN and ensemble

classifiers. Ten-fold cross-validation was used for classification. Table 2 shows the IMPE feature classification results for the unilateral fine motor imagery EEG data of 20 healthy people. The bold part of the table shows the highest classification accuracy of different participants for different classifiers.

Table 2. Classification accuracy of IMPE features for various classifiers (unit: %).

Participants	Tree	LDA	Naive Bayes	SVM	KNN	Ensemble
Sub01	47.5	48.3	49.2	53.3	**56.7**	47.5
Sub02	**60**	52.5	55.8	56.7	54.2	55.8
Sub03	48.3	50.8	50.8	50.8	**55**	50
Sub04	60.8	48.3	45.8	60	63.3	**64.2**
Sub05	55.8	51.7	52.5	51.7	50	**60**
Sub06	60.8	65.8	**67.5**	63.3	65.8	60.8
Sub07	45	55.8	53.3	**58.3**	51.7	56.7
Sub08	50	60.8	60.8	**61.7**	59.2	60.8
Sub09	**60.8**	55	47.5	52.5	53.3	54.2
Sub10	53.3	54.2	54.2	53.3	**55.8**	55
Sub11	46.7	45	41.7	44.2	**53.3**	43.3
Sub12	52.5	52.5	45	**56.7**	51.7	53.3
Sub13	**66.7**	63.3	63.3	62.5	60.8	63.3
Sub14	51.7	59.2	55.8	58.3	**60.8**	**60.8**
Sub15	59.2	**65.8**	62.5	65	63.3	**65.8**
Sub16	52.5	51.7	45.8	50.8	**53.3**	51.7
Sub17	56.7	59.2	60.8	60	60.8	**63.3**
Sub18	58.3	56.7	55	56.7	54.2	**60**
Sub19	51.7	**57.5**	46.7	56.7	**57.5**	55.8
Sub20	55.8	58.3	**60.8**	60	58.3	58.3
Mean	**54.71**	**55.62**	**53.74**	**56.63**	**56.95**	**57.03**

Figure 4 shows the average classification accuracy of the IMPE features of all subjects for the six classifiers.

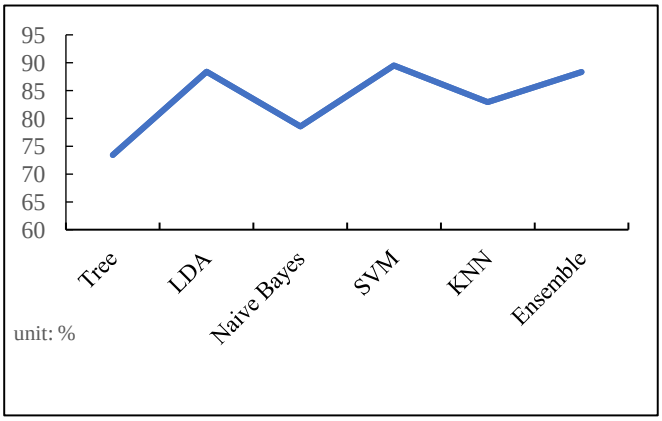

Figure 4. Average classification accuracy of IMPE features for all subjects.

It can be seen in Table 2 that, when the scale factor was set to 3, the overall classification accuracy of all subjects was low and the classification accuracy of Subject 6 reached the highest at 67.5%. The average classification accuracy of the six classifiers was the highest at 57.03%. The small number of single-subject samples shows the low classification accuracy of the IMPE features. When IMPE was used alone, the problem of low sensitivity to EEG data was magnified.

4.3. Multi-domain feature fusion and classification

The multi-domain feature matrix was obtained by fusing the spatial-based CSP features with the entropy-based IMPE features. The feature matrix was put into the Tree, LDA, Naive Bayes, SVM, KNN and ensemble classifiers for training and classification. Ten-fold cross-validation was used for classification. Table 3 shows the multi-domain feature classification results for the unilateral fine motor imagery EEG data of 20 healthy subjects. The bold part of the table shows the highest classification accuracy of different participants for different classifiers.

Table 3. Classification accuracy of fusion features for multiple classifiers (unit: %).

Participants	Tree	LDA	Naive Bayes	SVM	KNN	Ensemble
Sub01	69.2	93.3	81.7	**94.2**	91.7	91.7
Sub02	63.3	80.8	73.3	**90**	81.7	85
Sub03	70	79.2	65.8	**80.8**	69.2	77.5
Sub04	75	95	87.5	96.7	90	**97.5**
Sub05	69.2	85	65	**91.7**	72.5	87.5
Sub06	68.3	**80.8**	70	80	75.8	77.5
Sub07	67.5	**82.5**	66.7	76.7	67.5	80
Sub08	80.8	**99.2**	98.3	**99.2**	98.3	**99.2**
Sub09	76.7	85	78.3	**88.3**	82.5	86.7
Sub10	75	80.8	71.7	80	72.5	**85**
Sub11	73.3	**93.3**	78.3	90	89.2	91.7
Sub12	73.3	**90.8**	78.3	88.3	82.5	87.5
Sub13	76.7	**96.7**	80	95.8	86.7	94.2
Sub14	71.7	90.8	88.3	90.8	85.8	**92.5**
Sub15	73.3	95	**97.5**	95	94.2	95
Sub16	84.2	89.2	84.2	**93.3**	83.3	82.5
Sub17	78.3	98.3	90.8	**99.2**	94.2	**99.2**
Sub18	77.5	90	73.3	**92.5**	82.5	90
Sub19	69.2	81.7	65	80	76.7	**83.3**
Sub20	75.8	80.8	76.7	**87.5**	81.7	82.5
Mean	**73.42**	**88.41**	**78.54**	**89.5**	**82.93**	**88.3**

Figure 5 shows the average classification accuracy of the fusion features of all subjects for the six classifiers.

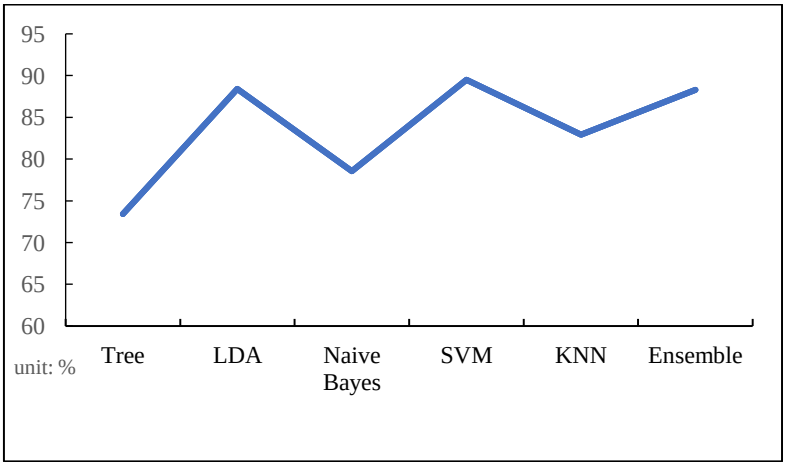

Figure 5. Average classification accuracy of fusion features for all subjects.

According to Table 3, the proposed multi-domain feature fusion algorithm achieved good results, with the highest classification accuracy of 99.2%. Compared with the CSP feature classification results, the highest average classification accuracy improvement of the same classifier was 1.52%. Compared with the result of IMPE feature classification, the average classification accuracy improvement of the same classifier was the highest at 32.87%. It can be seen that, when the CSP and IMPE were combined, the classification results for unilateral fine motor imagination were significantly improved. Fusing features from different domains can compensate for the lack of a single feature, and the interpretation of EEG signals will be more precise.

Figure 6 shows the confusion matrix diagram for the CSP feature, IMPE feature and multi-domain feature fusion of Subject 8. The diagram shows that the proposed multi-domain feature fusion algorithm had improved the accuracy relative to that of the single feature. Figure 7 shows the receiver operating characteristic (ROC) curves for CSP, IMPE and multi-domain feature fusion. According to the figure, the area under the curve values for CSP, IMPE and multi-domain feature fusion were 0.983, 0.590 and 0.992, respectively.

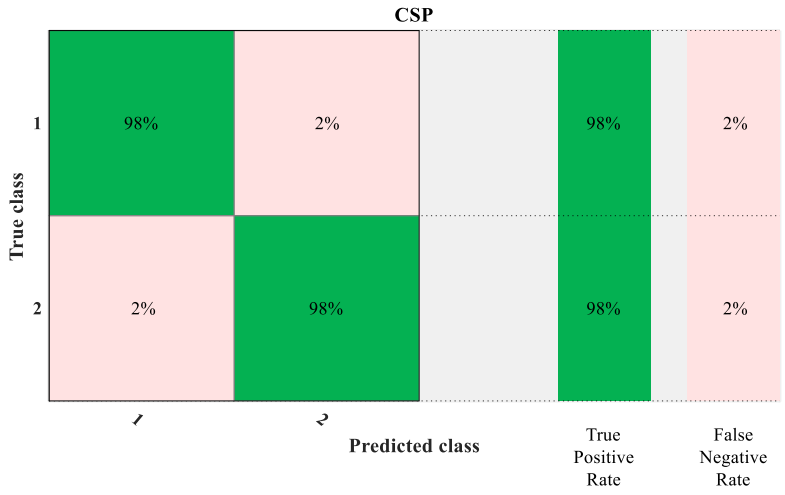

(a)

Continued on next page

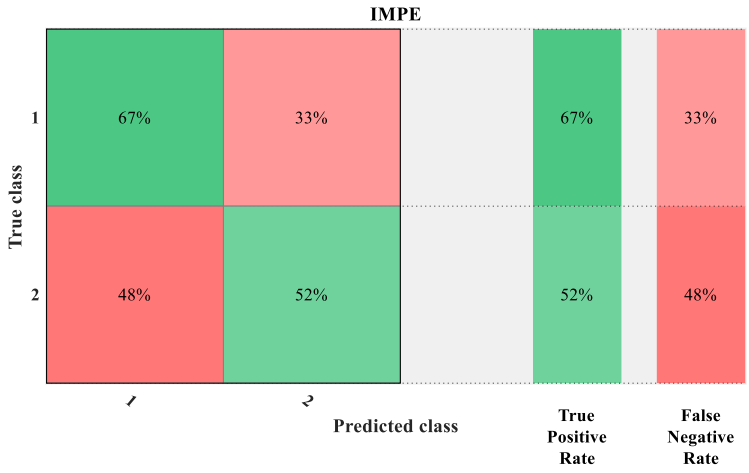

(b)

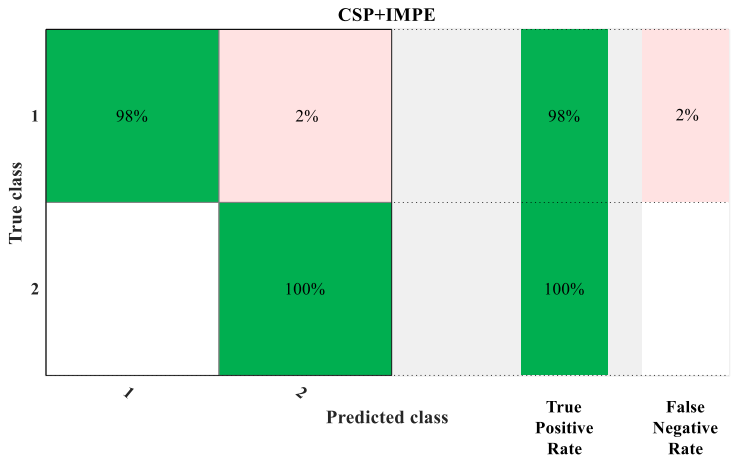

(c)

Figure 6. Confusion matrix for different features: (a) confusion matrix for CSP features; (b) confusion matrix for IMPE features; (c) confusion matrix for multi-domain fusion features.

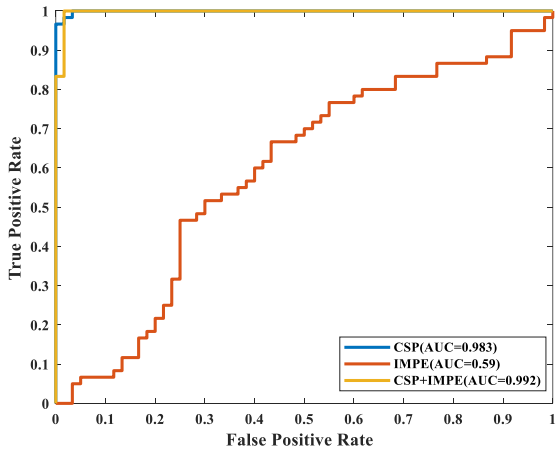

Figure 7. ROC curves for different feature extraction algorithms.

In order to evaluate the reliability of the feature extraction algorithm, the Kappa value was used as the evaluation index in this study. The Kappa value can be used to measure the classification accuracy and eliminate the disadvantages of random classification. The Kappa value is calculated using the following formula:

$$Kappa = \frac{P_0 - P_e}{1 - P_e} \tag{4.1}$$

P_0 is the subject's classification accuracy and P_e is the random classification accuracy. Since the unilateral fine motor imagery paradigm for upper limbs designed in this study is dichotomous, the P_e value was 0.5.

Figure 8 shows the highest classification rate and Kappa value for all subjects. As can be seen in the figure, the highest classification accuracy among subjects was 0.992, and the Kappa value was 0.984. It proves the superiority of the proposed multi-domain fusion feature extraction algorithm on fine motor imagery EEG data.

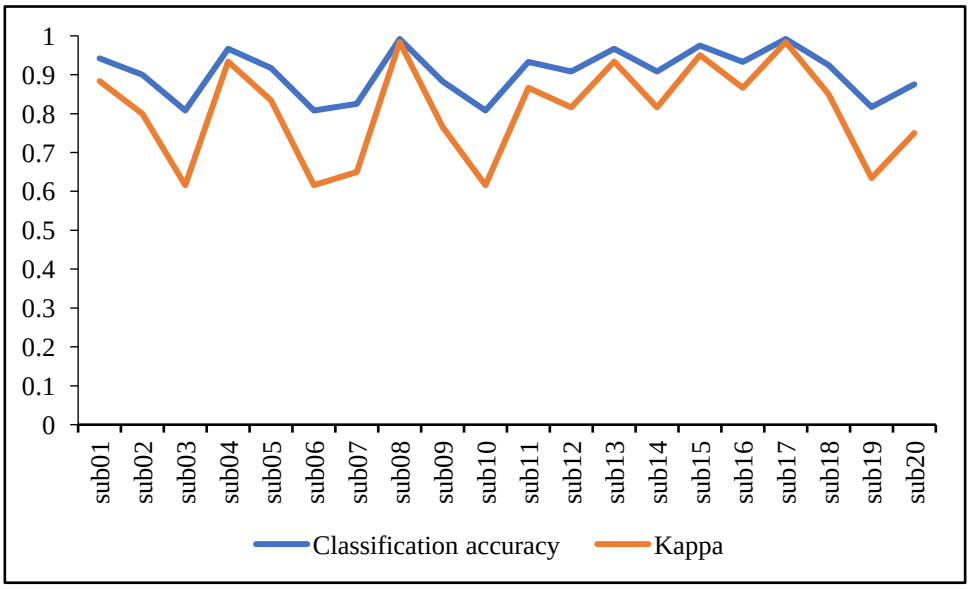

Figure 8. Classification accuracy and Kappa values of all subjects.

4.4. Comparison with existing studies

The common time-frequency-spatial patterns (CTFSP) [31] algorithm was selected to compare the classification accuracy with the self-collected fine motor imagery EEG data and the proposed multi-domain fusion features. As shown in Table 4, the highest classification rate and Kappa value for CTFSP, as obtained by using the self-collected data in this study, were compared with the multi-domain fusion feature extraction algorithm.

Table 4. Comparison of accuracy (ACC) and Kappa values for CTFSP and fusion features.

	CTFSP		Multiple-domain fusion	
	ACC (%)	Kappa	ACC (%)	Kappa
sub01	90.8	0.816	94.2	0.884
sub02	92.5	0.85	90	0.8
sub03	75	0.5	80.8	0.616
sub04	86.7	0.734	96.7	0.934
sub05	96.7	0.934	91.7	0.834
sub06	85.8	0.716	80.8	0.616
sub07	78.3	0.566	82.5	0.65
sub08	79.2	0.584	99.2	0.984
sub09	98.3	0.966	88.3	0.766
sub10	89.2	0.784	80.8	0.616
sub11	91.7	0.834	93.3	0.866
sub12	91.7	0.834	90.8	0.816
sub13	96.7	0.934	96.7	0.934
sub14	87.5	0.75	90.8	0.816
sub15	97.5	0.95	97.5	0.95
sub16	97.5	0.95	93.3	0.866
sub17	92.5	0.85	99.2	0.984
sub18	96.7	0.934	92.5	0.85
sub19	91.7	0.834	81.7	0.634
sub20	81.7	0.634	87.5	0.75
Mean	**89.885**	**0.7977**	**90.415**	**0.8083**

As can be seen in the above table, the proposed multi-domain fusion feature extraction algorithm has certain advantages over the CTFSP algorithm. The average accuracy and average Kappa values for the proposed method were 0.53% and 0.0106 higher than those obtained via the CTFSP algorithm, respectively.

5. Discussion

The multi-domain feature fusion algorithm combining the spatial domain and the entropy domain was used to extract features from the EEG data of unilateral fine motor imagery, which was significantly improved relative to the single-domain feature extraction method.

In this study, CSP features were extracted from the spatial domain, IMPE features were extracted from the entropy domain and multi-domain features were extracted. The highest classification accuracies were 98.3, 67.5 and 99.2%, respectively. Compared with CSP feature classification results, the average classification accuracy improvement of the same classifier was 1.52%. Compared with the result of IMPE feature classification, the average classification accuracy improvement of the same classifier was the highest at 32.87%. Compared with existing studies, Hou et al. [32] proposed to combine the CSP with the dual spectrum and Shannon entropy, and the improvement rates after feature fusion were 2.05, 24.85 and 20.18%, respectively. Hu et al. [33] proposed a method combining WOSF

and MSE, which improved the average accuracy by 9.4%.

The multi-domain feature fusion algorithm applies the high sensitivity of the CSP for motor imagery feature extraction to make up for the low sensitivity and high time cost of IMPE alone, and it uses the reliability of IMPE to make up for the inadaptability of the CSP when the number of leads was small.

There are still some deficiencies in the study of unilateral fine motor imagery. The unilateral fine motor imagery designed in this study is limited to the movement of a single joint. In contrast, in daily life, every movement of healthy people often combines more than two joints. Hence, subsequent research needs to combine multiple unilateral joint data. The classifiers used in this study are still classical classifiers, and some improved classifiers should be considered to measure the extracted motor imagery features in subsequent studies, such as the combination of ensemble learning and an attention mechanism [34], LS-SVM [35], etc. After expanding enough self-collected datasets, an attention network [36] can be used to further explore the feature extraction of fine motor imagery EEG data. In future studies, it is necessary to further compare the multi-domain fusion feature extraction algorithm proposed in this paper with SOTA models.

6. Conclusions

The classical motor imagery paradigm cannot meet the needs of rehabilitation training for patients after stroke, and a paradigm for fine joint motor training has emerged. This study involved the design of a fine motor imagery paradigm for unilateral rehabilitation training of the shoulder and elbow joints and the use of a Neuracle EEG acquisition device to collect EEG data from 20 healthy people.

The preprocessed EEG data were extracted by using the CSP algorithm in the spatial domain and IMPE algorithm in the entropy domain. The features of the two domains were fused to obtain the highest classification accuracies of 98.3, 67.5 and 99.2%, respectively. The results show that the multi-domain feature fusion algorithm can complement the advantages of the feature extraction algorithms between different domains to a certain extent, and our results prove that the multi-domain feature extraction algorithm has a noticeable effect on the discrimination of unilateral fine motor imagery tasks, which provides a new means of rehabilitation training for affected limb rehabilitation after stroke.

Acknowledgments

This work was partly supported by the Jiangsu Key Research and Development Plan (BE2021012-2 and BE2021012-5), Key Laboratory of Brain Machine Collaborative Intelligence Foundation of Zhejiang Province (2020E10010-04), Human-Machine Intelligence and Interaction International Joint Laboratory Project, Changzhou Sci & Tech Program (CE20215026 and CE20225034) and Postgraduate Research & Practice Innovation Program of Jiangsu Province (SJCX21_1289 and KYCX22_3058).

Conflict of interest

All authors have no conflicts of interest.

References

1. S. Aggarwal, N. Chugh, Signal processing techniques for motor imagery brain computer interface: a review, *Array*, **1–2** (2019), 100003. https://doi.org/10.1016/j.array.2019.100003
2. B. Yang, J. Ma, W. Qiu, Y. Zhu, X. Meng, A new 2-class unilateral upper limb motor imagery tasks for stroke rehabilitation training, *Med. Novel Technol. Devices*, **13** (2022), 100100. https://doi.org/10.1016/j.medntd.2021.100100
3. M. A. Cervera, S. R. Soekadar, J. Ushiba, J. del R. Millán, M. Liu, N. Birbaumer, et al., Brain-computer interfaces for post-stroke motor rehabilitation: a meta-analysis, *Ann. Clin. Transl. Neurol.*, **5** (2018), 651–663. https://doi.org/10.1002/acn3.544
4. U. Chaudhary, N. Birbaumer, A. Ramos-Murguialday, Brain-computer interfaces for communication and rehabilitation, *Nat. Rev. Neurol.*, **12** (2016), 513–525. https://doi.org/10.1038/nrneurol.2016.113
5. R. Mane, T. Chouhan, C. Guan, BCI for stroke rehabilitation: motor and beyond, *J. Neural Eng.*, **17** (2020), 041001. https://doi.org/10.1088/1741-2552/aba162
6. H. Dose, J. S. Møller, H. K. Iversen, S. Puthusserypady, An end-to-end deep learning approach to MI-EEG signal classification for BCIs, *Expert Syst. Appl.*, **114** (2018), 532–542. https://doi.org/10.1016/j.eswa.2018.08.031
7. Y. Zhang, W. Chen, C. L. Lin, Z. Pei, J. Chen, Z. Chen, Boosting-LDA algriothm with multi-domain feature fusion for motor imagery EEG decoding, *Biomed. Signal Process. Control*, **70** (2021), 102983. https://doi.org/10.1016/j.bspc.2021.102983
8. A. Khalaf, E. Sejdic, M. Akcakaya, Common spatial pattern and wavelet decomposition for motor imagery EEG- fTCD brain-computer interface, *J. Neurosci. Methods*, **320** (2019), 98–106. https://doi.org/10.1016/j.jneumeth.2019.03.018
9. P. Gaur, H. Gupta, A. Chowdhury, K. McCreadie, R. B. Pachori, H. Wang, A sliding window common spatial pattern for enhancing motor imagery classification in EEG-BCI, *IEEE Trans. Instrum. Meas.*, **70** (2021), 1–9. https://doi.org/10.1109/TIM.2021.3051996
10. Y. Zhang, C. S. Nam, G. Zhou, J. Jin, X. Wang, A. Cichocki, Temporally constrained sparse group spatial patterns for motor imagery BCI, *IEEE Trans. Cybern.*, **49** (2019) 3322–3332. https://doi.org/10.1109/TCYB.2018.2841847
11. N. S. Malan, S. Sharma, Motor imagery EEG spectral-spatial feature optimization using dual-tree complex wavelet and neighbourhood component analysis, *IRBM*, **43** (2022), 198–209. https://doi.org/10.1016/j.irbm.2021.01.002
12. K. K. Ang, Z. Y. Chin, H. Zhang, C. Guan, Filter Bank Common Spatial Pattern (FBCSP) in brain-computer interface, in *2008 IEEE International Joint Conference on Neural Networks (IEEE World Congress on Computational Intelligence)*, (2008), 2390–2397. https://doi.org/10.1109/IJCNN.2008.4634130
13. K. Sivasankari, K. Thanushkodi, An improved EEG signal classification using neural network with the consequence of ICA and STFT, *J. Electr. Eng. Technol.*, **9** (2014), 1060–1071. https://doi.org/10.5370/JEET.2014.9.3.1060
14. M. Diykh, Y. Li, P. Wen, EEG sleep stages classification based on time domain features and structural graph similarity, *IEEE Trans. Neural Syst. Rehabil. Eng.*, **24** (2016), 1159–1168. https://doi.org/10.1109/TNSRE.2016.2552539

15. N. K. Al-Qazzaz, M. K. Sabir, S. H. B. M. Ali, S. A. Ahmad, K. Grammer, Multichannel optimization with hybrid spectral- entropy markers for gender identification enhancement of emotional-based EEGs, *IEEE Access*, **9** (2021), 107059–107078. https://doi.org/10.1109/ACCESS.2021.3096430
16. N. Mammone, F. La Foresta, F. C. Morabito, Automatic artifact rejection from multichannel scalp EEG by wavelet ICA, *IEEE Sens. J.*, **12** (2012), 533–542. https://doi.org/10.1109/JSEN.2011.2115236
17. X. Liu, G. Wang, J. Gao, Q. Gao, A quantitative analysis for EEG signals based on modified permutation-entropy, *IRBM*, **38** (2017), 71–77. https://doi.org/10.1016/j.irbm.2017.02.001
18. D. Q. Phung, D. Tran, W. Ma, P. Nguyen, T. Pham, Using shannon entropy as EEG signal feature for fast person identification, *ESANN*, **4** (2014), 413–418.
19. X. Jie, R. Cao, L. Li, Emotion recognition based on the sample entropy of EEG, *Bio-Med. Mater. Eng.*, **24** (2014), 1185–1192. https://doi.org/10.3233/BME-130919
20. Y. Park, W. Chung, Optimal channel selection using correlation coefficient for CSP based EEG classification, *IEEE Access*, **8** (2020), 111514–111521. https://doi.org/10.1109/ACCESS.2020.3003056
21. X. Liu, Y. Shen, J. Liu, J. Yang, P. Xiong, F. Lin, Parallel spatial–temporal self-attention CNN-based motor imagery classification for BCI, *Front. Neurosci.*, **14** (2020), 587520. https://doi.org/10.3389/fnins.2020.587520
22. Y. A. Baysal, S. Ketenci, I. H. Altas, T. Kayikcioglu, Multi-objective symbiotic organism search algorithm for optimal feature selection in brain computer interfaces, *Expert Syst. Appl.*, **165** (2021), 113907. https://doi.org/10.1016/j.eswa.2020.113907
23. Z. Yu, W. Chen, T. Zhang, Motor imagery EEG classification algorithm based on improved lightweight feature fusion network, *Biomed. Signal Process. Control*, **75** (2022), 103618. https://doi.org/10.1016/j.bspc.2022.103618
24. C. Wang, Y. Wu, C. Wang, Y. Zhu, C. Wang, Y. Niu, et al., MI-EEG classification using Shannon complex wavelet and convolutional neural networks, *Appl. Soft Comput.*, **130** (2022), 109685. https://doi.org/10.1016/j.asoc.2022.109685
25. A. Jafarifarmand, M. A. Badamchizadeh, Real-time multiclass motor imagery brain-computer interface by modified common spatial patterns and adaptive neuro-fuzzy classifier, *Biomed. Signal Process. Control*, **57** (2020), 101749. https://doi.org/10.1016/j.bspc.2019.101749
26. X. Zheng, J. Li, H. Ji, L. Duan, M. Li, Z. Pang, et al., Task transfer learning for EEG classification in motor imagery-based BCI system, *Comput. Math. Methods Med.*, **2020** (2020), e6056383. https://doi.org/10.1155/2020/6056383
27. Y. Xu, Q. Wei, H. Zhang, R. Hu, J. Liu, J. Hua, et al., Transfer learning based on regularized common spatial patterns using cosine similarities of spatial filters for motor-imagery BCI, *J. Circuits Syst. Comput.*, **28** (2019), 1950123. https://doi.org/10.1142/S0218126619501238
28. M. Z. Baig, N. Aslam, H. P. H. Shum, L. Zhang, Differential evolution algorithm as a tool for optimal feature subset selection in motor imagery EEG, *Expert Syst. Appl.*, **90** (2017), 184–195. https://doi.org/10.1016/j.eswa.2017.07.033
29. H. Azami, J. Escudero, Improved multiscale permutation entropy for biomedical signal analysis: interpretation and application to electroencephalogram recordings, *Biomed. Signal Process. Control*, **23** (2016), 28–41. https://doi.org/10.1016/j.bspc.2015.08.004

30. M. E. S. H. Jomaa, P. Van Bogaert, N. Jrad, N. E. Kadish, N. Japaridze, M. Siniatchkin, et al., Multivariate improved weighted multiscale permutation entropy and its application on EEG data, *Biomed. Signal Process. Control*, **52** (2019), 420–428. https://doi.org/10.1016/j.bspc.2018.08.004
31. Y. Miao, J. Jin, I. Daly, C. Zuo, X. Wang, A. Cichocki, et al., Learning common time-frequency-spatial patterns for motor imagery classification, *IEEE Trans. Neural Syst. Rehabil. Eng.*, **29** (2021), 699–707. https://doi.org/10.1109/TNSRE.2021.3071140
32. Y. Hou, T. Chen, X. Lun, F. Wang, A novel method for classification of multi-class motor imagery tasks based on feature fusion, *Neurosci. Res.*, **176** (2022), 40–48. https://doi.org/10.1016/j.neures.2021.09.002
33. L. Hu, J. Xie, C. Pan, X. Wu, D. Hu, Multi-feature fusion method based on WOSF and MSE for four-class MI EEG identification, *Biomed. Signal Process. Control*, **69** (2021), 102907. https://doi.org/10.1016/j.bspc.2021.102907
34. Y. Djenouri, A. Belhadi, A. Yazidi, G. Srivastava, J. C. W. Lin, Artificial intelligence of medical things for disease detection using ensemble deep learning and attention mechanism, *Expert Syst.*, **e13093** (2022). https://doi.org/10.1111/exsy.13093
35. T. Zhang, W. Chen, M. Li, Classification of inter-ictal and ictal EEGs using multi-basis MODWPT, dimensionality reduction algorithms and LS-SVM: a comparative study, *Biomed. Signal Process. Control*, **47** (2019), 240–251. https://doi.org/10.1016/j.bspc.2018.08.038
36. W. Pan, Y. An, Y. Guan, J. Wang, MCA-net: a multi-task channel attention network for Myocardial infarction detection and location using 12-lead ECGs, *Comput. Biol. Med.*, **150** (2022), 106199. https://doi.org/10.1016/j.compbiomed.2022.106199

AIMS Press